CDF/PUB/CDFR/PUBLIC/8378
Draft 2.0
July 27, 2006

Search for Heavy, Long-Lived Particles that Decay to Photons at CDF

CDF Collaboration

Abstract

We present the results of a search for heavy, long-lived particles that decay to photons in a sample of γ+$\not\!\!E_{\rm T}$+Jet events at CDF Run II. Candidate events are selected based on the delayed arrival time of the photon at the calorimeter as measured with the timing system recently installed on the electromagnetic calorimeter. We find 10 events using 570 pb^{-1} in data, consistent with the background estimate of 7.6$\pm$1.9 events. We show exclusion regions and set limits on GMSB models with the delayed photons via long-lived neutralinos with the decay mode $\tilde{\chi}_1^0 \rightarrow \gamma \tilde{G}$.

1 Introduction

Since the Standard Model (SM) is known to be incomplete [1], there is a wide program at the Tevatron to look for hints of new physics. The recently commissioned timing system installed on the CDF electromagnetic calorimeter, known as the EMTiming system [2], has now taken enough data that it gives new sensitivity to heavy, long-lived particles that decay to photons [3].

Gauge Mediated Supersymmetry Breaking models [4] are an example theory that can produce such particles as long-lived neutralinos can decay into photons and missing transverse energy ($\not\!\!E_{\rm T}$) like the $ee\gamma\gamma\not\!\!E_{\rm T}$ candidate event [5]. At the Tevatron the cross section is dominated by gaugino pair production (Figure 1), resulting in a pair of neutralinos in association with other final state particles that can be identified in the calorimeter, for example, as jets. The lightest neutralino ($\tilde{\chi}_1^0$) is the next- to- lightest supersymmetric particle (NLSP) and decays into a photon and a gravitino ($\tilde{G}$), which is the lightest supersymmetric particle (LSP). The $\tilde{G}$ escapes the detector undetected and gives rise to $\not\!\!E_{\rm T}$. Previous searches have been performed for such models in the $\gamma\gamma\not\!\!E_{\rm T}$ final state.

In GMSB models, the lifetime of the neutralino is a free parameter, and can be quite large. Since the neutralino can travel a significant distance before decaying, the neutralino could leave the detector completely without interacting, or if it decays in the detector could produce a photon that would appear to be arriving at the face of

the calorimeter with a slight delay relative to the expectation for promptly produced photons. This is shown in Figure 2. If the neutralino has a lifetime of the order of $O(10)$ ns, previous studies have indicated that the highest sensitivity to such a model comes from final state signatures consisting of a photon with a delayed arrival time, one or more energetic jets, and $\not\!\!E_{\rm T}$ [3].

We present the first direct search at the Tevatron for heavy, long- lived particles that decay to photons in the γ+$\not\!\!E_{\rm T}$+Jet final state using the CDF Run II detector and 570 pb^{-1} of data. For concreteness we focus on GMSB models with the Snowmass Slope constraint (SPS 8) [6] to quote results as a function of $\tilde{\chi}_1^0$ mass and lifetime. While GMSB provides model-dependent limits, by keeping our topological cuts to a minimum we keep a quasi model- independent/signature-based approach in our search, as well as providing a useful benchmark to compare our sensitivity with other searches at LEP [7].

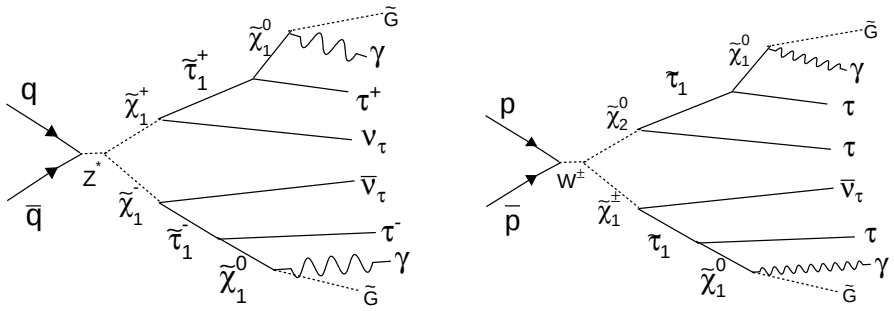

Figure 1: The Feynman diagrams for the two leading GMSB processes. The final state $\tilde{G}$ leaves the detector undetected producing missing transverse energy, $\not\!\!E_{\rm T}$. We require a jet that can be either the tau particle decaying either hadronically or electronically, or the second photon. Other processes, such as slepton pair production, can also contribute to the acceptance.

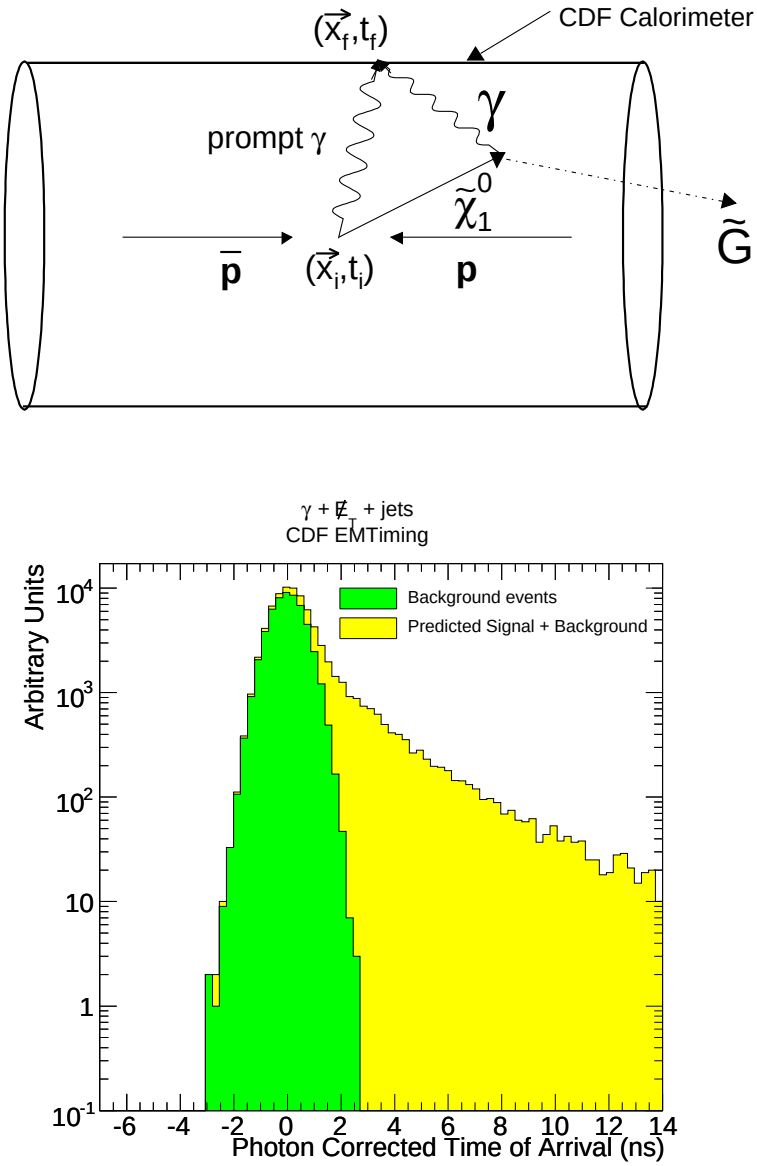

Figure 2: On the top: the decay of the heavy particle into a photon and a gravitino. It takes the photon more time to reach the detector compared to the photon from the collision point. On the bottom: A toy Monte Carlo signal simulation of the Standard Model background and the signal. The green shaded region is the Standard Model, and the photon corrected time is normalized to the expected time of arrival, thus it is zero and smeared by the timing resolution (0.65 ns). The yellow is the expectation from GMSB SUSY and has a significant fraction of the events which are well separated from zero, as expected from the neutralino decaying in flight.

2 Data Selection

The analysis selection begins with events that pass the CDF trigger by virtue of having a high energy photon-like EM cluster (presumably from our photon) in the central portion of the detector, $|\eta|$ <1.1, and large $\not\!\!E_{\rm T}$. The trigger is 100% efficient for the final, offline selected γ and $\not\!\!E_{\rm T}$ energies.

Offline, we select events with γ, $\not\!\!E_{\rm T}$, and a jet. Only the highest $E_{\rm T}$ photon is picked, while any second photon candidate would be counted as a jet. In this way we are sensitive to the signatures with one or both neutralinos decaying inside the detector. We apply extra topological cuts to reduce the contamination from QCD events with fake $\not\!\!E_{\rm T}$, cosmic rays, and beam halo effects. These cuts are listed, along with the full data selection criteria in Table 1. In particular we note that the cut on $\Delta\phi$ between a photon and the leading jet rejects QCD events where a jet is poorly measured and causes $\not\!\!E_{\rm T}$. We also pick the highest $\sum P_{\rm T}$ vertex in the event and require it to have 4 or more tracks with total $\sum P_{\rm T}$>10 GeV to reduce beam halo and cosmics contamination since those backgrounds are not correlated with a collision. The final cut on the corrected time of arrival of the photon is discussed in more detail in Section 4 after a discussion of the backgrounds and the optimization procedure.

Quality Cuts: γ $E_T > 30$ GeV $\|\eta\|$ <1.1	ϵ(%)
Photon ID and Fiducial	74
Cosmic Rejection:	
$\Delta\phi > 30^0$ between γ and trackless μ stub	98
Collision Fiducial	95
Baseline Cuts	
Photon $\|\eta\|$ <1.1 $E_T > 30$ GeV, $\not\!\!E_{\rm T} > 30$ GeV	41
Good Vertex (4 or more tracks, $\sum P_{\rm T}$>10 GeV)	40
Jet $E_T^{\rm jet}$(cone 0.7) > 30 GeV, $\|\eta^{\rm jet}_{\rm detector}\| < 2.0$	27
Optimized Cuts	
$\not\!\!E_{\rm T} > 50$ GeV	19
$\Delta\phi(\not\!\!E_{\rm T}$,Jet) > 0.5 rad	18
1.5 ns < $t_{arrival}$ < 10 ns	7

Table 1: The data selection criteria and the total event efficiency. We note that the top three cuts are estimated from data and should be model-independent. The lower set of cuts are model-dependent and are estimated using a Monte Carlo simulation, discussed in Section 4, for an example mass point at $m_\chi = 93.6$ GeV and lifetime of 10 ns. The efficiency is given cumulatively, as a function of the cuts.

3 Backgrounds

There are two major sources of the backgrounds: collision and non-collision photon candidates. Collision photons are presumed to be from the Standard Model interactions (e.g. γ+ j+Fake $\not\!\!E_{\rm T}$; jj+Fake $\not\!\!E_{\rm T}$, j fakes γ; $W \rightarrow e\nu$, electron fakes γ). The non-collision photon candidates are produced by cosmic rays and beam effects. Cosmic rays are not correlated in time with collisions, and therefore their timing shape, as we will show later, is flat in time. The photon candidates from beam halo have negative time. We use events in the time regions that do not overlap with prompt photons to estimate the overall non-collision backgrounds. All three are estimated using data.

A full description of the EMTiming system as well as its timing resolution and various effects can be found in [2]. The timing distribution shape for collision events is estimated from $W \rightarrow e\nu$ data where the electron track is dropped from the vertexing to closely mimic events with photons. Of particular importance is that the arrival time is corrected for the expected photon path from the collision vertex position and time (estimated from COT tracks to have an RMS of 1.3 ns). The result, shown in Figure 3, is a double Gaussian centered at zero with the primary RMS=0.64 ns and the secondary RMS=2.05 ns. This shape can be understood as coming from when the photon timing is associated with the correct primary vertex, and when it is associated with a vertex unrelated to the collision. The shape of each distribution does not depend on the kinematic cuts used to select the final sample, but the relative event fraction of right to wrong vertex can vary.

The timing distributions of non-collision photon candidates produced by cosmic rays and beam effects are shown in Figure 3 and are estimated from data using events with no track activity. The cosmic contribution is flat in time and drops near the edges of the energy integration gate. The beam halo photon candidates are produced by the muons flying parallel to the beam line. Relative to the nominal collision time they populate the negative region. Those events normally have a trail of the calorimeter towers with some energy deposited in the same wedge with the photon, the feature used to separate cosmic ray photons from beam halo. We use those shapes as the templates to estimate contributions from each of the backgrounds by fitting them to the events in the time windows not overlapping with the prompt or signal regions.

The number of events in our signal region is estimated using the non-collision templates and two Gaussians for prompt photons. As discussed later, we choose a final timing window of [1.5, 10] ns. To determine the expected backgrounds for this region we first normalize the non-collision templates to the events in window of [-30, -8] ns, dominated by beam halo, and in window of [30, 80] ns, dominated by cosmics. The relative normalization of the cosmic to beam halo template is allowed to float. Then we establish relative contributions of right to wrong vertex events by fitting events in the [-8, 1.2] ns window to the double Gaussian with the non-collision contribution subtracted. In this way the background estimate is Monte Carlo independent, and does not depend, to a high degree of approximation, on the actual SM sources, just their

total event rate which is estimated directly from data.

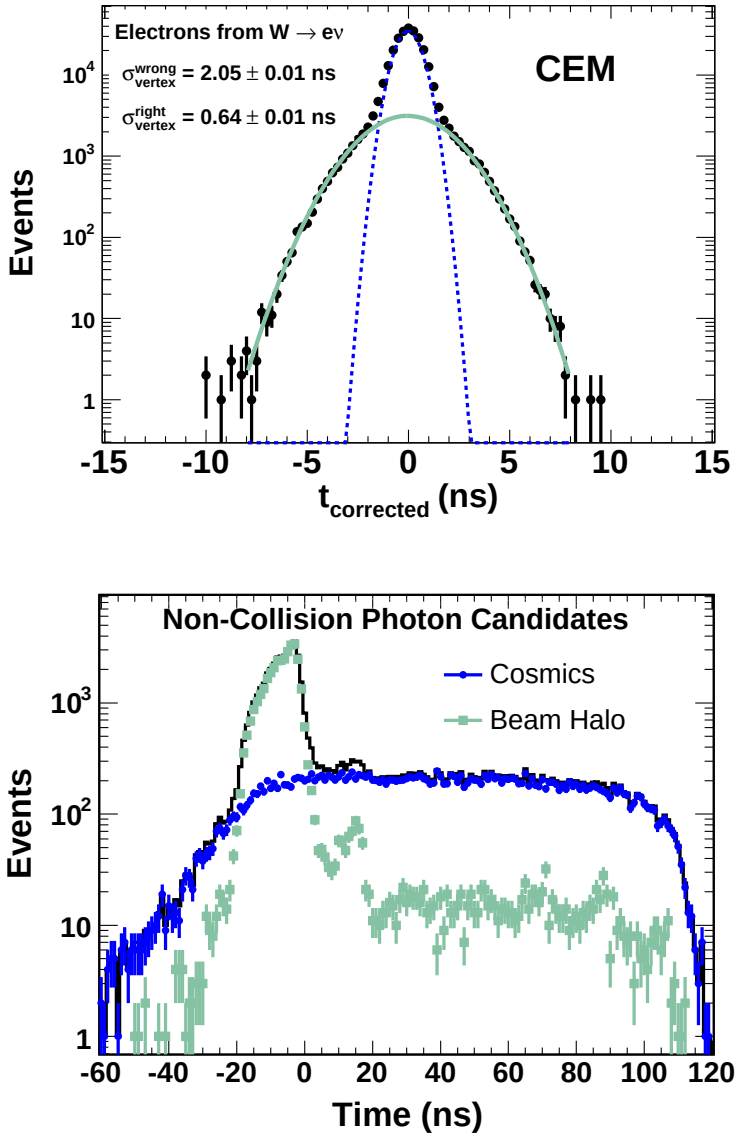

Figure 3: The background time shapes from collision and non-collision sources as estimated from data. The top plot shows the expected timing distribution for collision photons, estimated using a sample of $W \rightarrow e\nu$ events, with the collision time subtracted estimated from data samples. The primary Gaussian is for the cases when the correct vertex is picked, the secondary Gaussian is for the cases when the wrong vertex is picked. The bottom plot shows photon timing from beam halo and cosmic ray background sources, estimated from data events with zero track activity.

4 Signal Monte Carlo

The signal acceptance is estimated using a GMSB model with the Snowmass slopes [4] simulated with Pythia as well as a full detector simulation. In this scenario a $\tilde{\chi}_1^0$ is the NLSP and decays into a photon and a $\tilde{G}$, which is the lightest supersymmetric particle with a lifetime in the $O(10)$ ns range. We include all possible processes, not only the two leading ones shown in Figure 1.

The acceptance depends on a number of effects that are a function of both the $\tilde{\chi}_1^0$ lifetime and mass. As discussed in detail in Ref. [3], for an event to pass the final selection criteria, a $\tilde{\chi}_1^0$ must both decay in the detector and in such a way as to produce a delayed photon. Highly boosted $\tilde{\chi}_1^0$ typically do not contribute to the acceptance because not only does the boost extend the lifetime in the detector reference frame, making it more likely to leave the detector, a highly boosted $\tilde{\chi}_1^0$ that does decay in the detector typically will produce a photon flying in the original $\tilde{\chi}_1^0$ direction, thus making the decay-photon's arrival time indistinguishable from promptly produced photons. For small boosts, the decay is both more likely to occur in the detector, and to produce both the displaced decay position and extreme decay angles that translate into a larger delay for the photon, again see Figure 2a. Thus, for a given mass and lifetime combination, since there will be a distribution of boosts of the $\tilde{\chi}_1^0$ events will both produce photons with low and large arrival times, again see Figure 2b. These effects counter balance each other such that the total event acceptance at $\sim$0 ns is $\sim$0 (lots of photons produced in the detector, but none have large delay times), rises as a function of lifetime as more of the photons have larger delay times to a peak at around 5 ns, then falls as the fraction of neutralinos leaving the detector dominates. We note that the acceptance also increases, roughly linearly, as a function of mass as the boost effects are mitigated by the ability to produce highly boosted $\tilde{\chi}_1^0$ in the collision. Both of these will be seen later in Figures 7 and 8. For reference, the total signal acceptance is 7.3$\pm$0.7% for the GMSB point of the neutralino mass $m_\chi = 93.6$ GeV and lifetime $\tau_\chi = 10$ ns. The dominant systematic error contribution comes from the photon ID efficiency (5%) and on the uncertainty of the mean of the timing distribution(7%). Taking all errors in quadrature, and rounding up, we estimate a 10% systematic error.

Based on the expected number of events from the background estimation and on our understanding of the signal acceptance we perform an optimization of the cuts in order to achieve the minimum expected upper limit on the signal cross-section. The optimization results, as a function of the expected cross section limit, are shown in Figure 4 as a function of the final timing requirement. We note for completeness that the final set of kinematic requirements, shown in Table 1, are also optimized simultaneously.

5 Results

After estimating all backgrounds in the timing window of [1.5, 10] ns we open the blinded signal region and find 10 events. The number of expected events from all

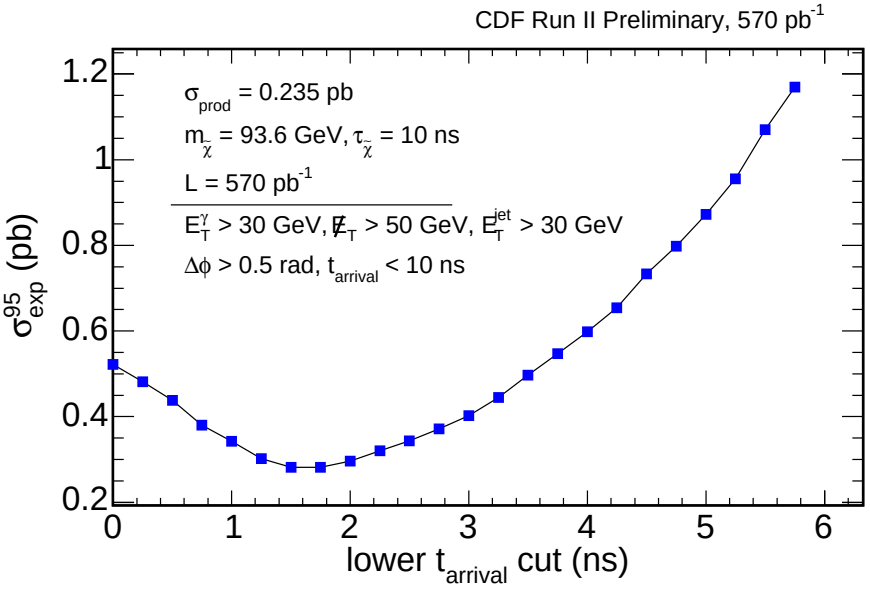

Figure 4: The expected 95% C.L. cross section limit as a function of the cutoff on the photon arrival time.

backgrounds is 7.6±1.9 events: 4.7±1.7 expected from collision photons, 2.2±0.7 from cosmic rays, and 0.7±0.2 from beam halo. The total systematic error on the prediction is dominated by the uncertainty on the timing parameters of the collision Gaussian. A comparison between data and background as a function of the photon arrival time is shown in Figure 5. Other kinematic distributions are shown in Figure 6, indicating that the data is well-modeled by the background only hypothesis.

The result is consistent with no-signal hypothesis, therefore we set limits on the neutralino lifetime and mass. Example cross section limits as a function of mass and lifetime are shown in Figure 7. The two dimensional exclusion region, taking into account the predicted production cross section, is shown in Figure 8. Since the number of observed events is slightly above expectations, the observed limits are slightly worse than the expected limits.

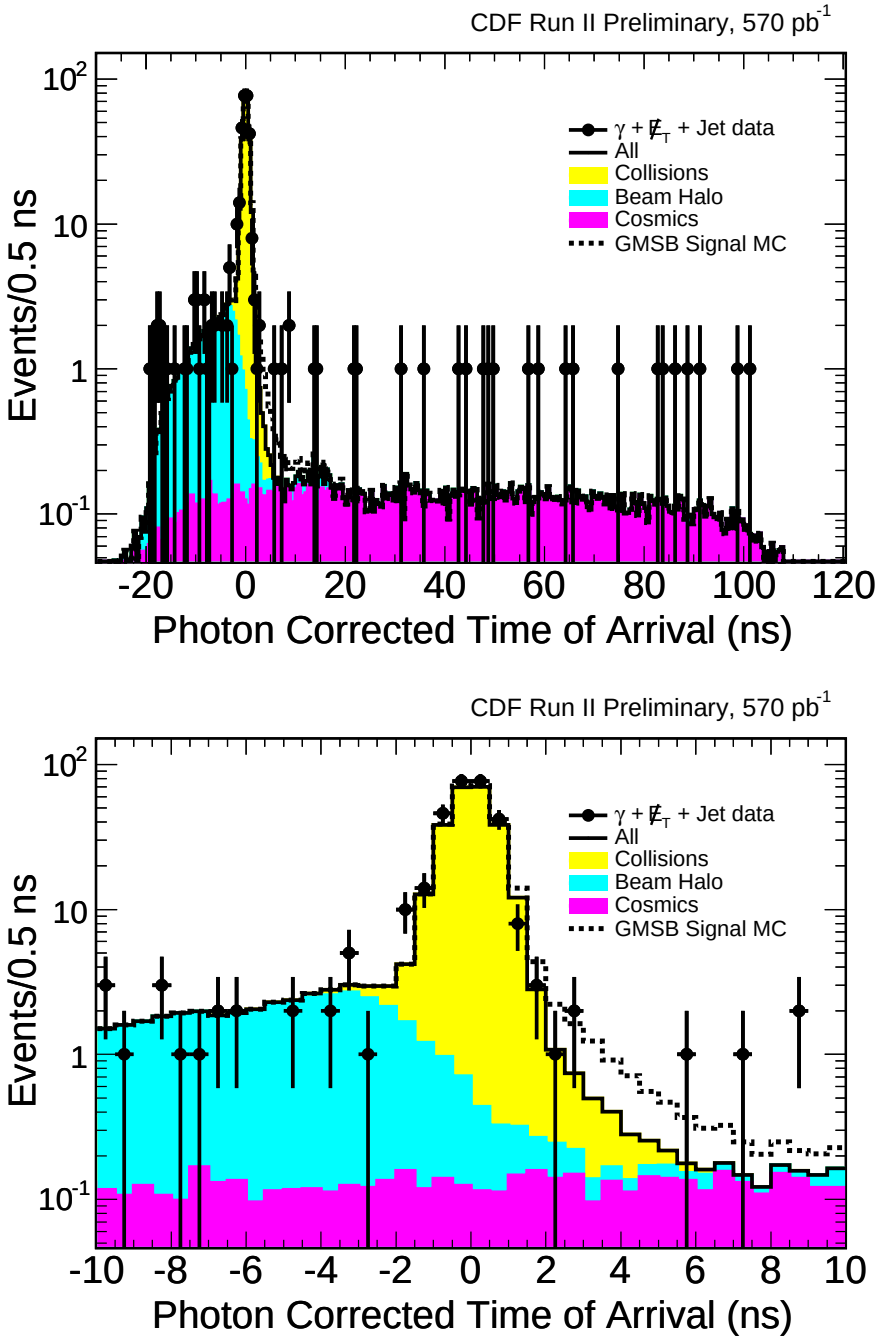

Figure 5: The predicted timing distribution for photons after all kinematic cuts. The top plot shows the full timing window and the bottom plot shows the same distributions, but for the region around the final signal region of 1.5< $t_{\text{corrected}}$ <10 ns. The GMSB signal is for an example point at $m_{\chi} = 93.6$ GeV and $\tau_{\chi} = 10$ ns and is normalized to the expected number of signal events 6.8±0.7. We predict 7.6±1.9 background events and observe 10 events..

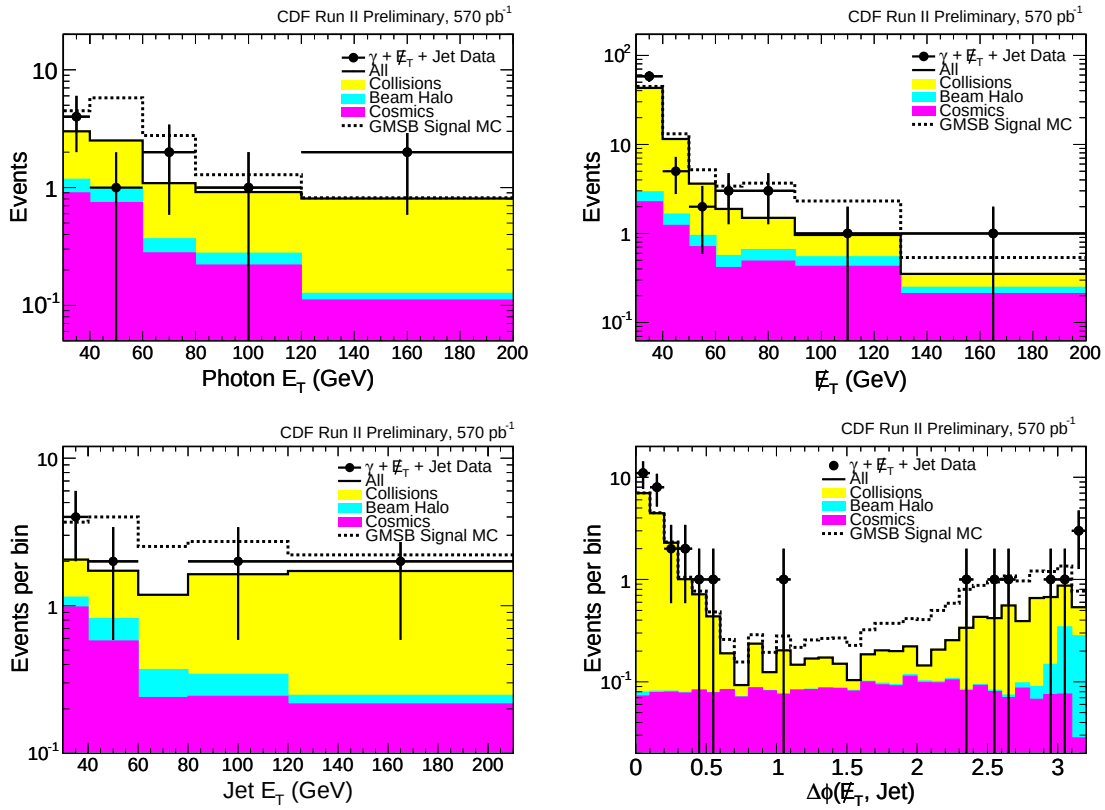

Figure 6: A comparison of the kinematic variables for the backgrounds, data and expected signal shapes. Note that all the distributions are well modeled by the data, indicating no evidence of new physics. Also note, that the final $\not\!\!E_{\rm T}$ cut is pushed from the 30 GeV cut indicated in the top right figure (trigger threshold) to 50 GeV in the final analysis; all other plots assume $\not\!\!E_{\rm T}$>50 GeV.

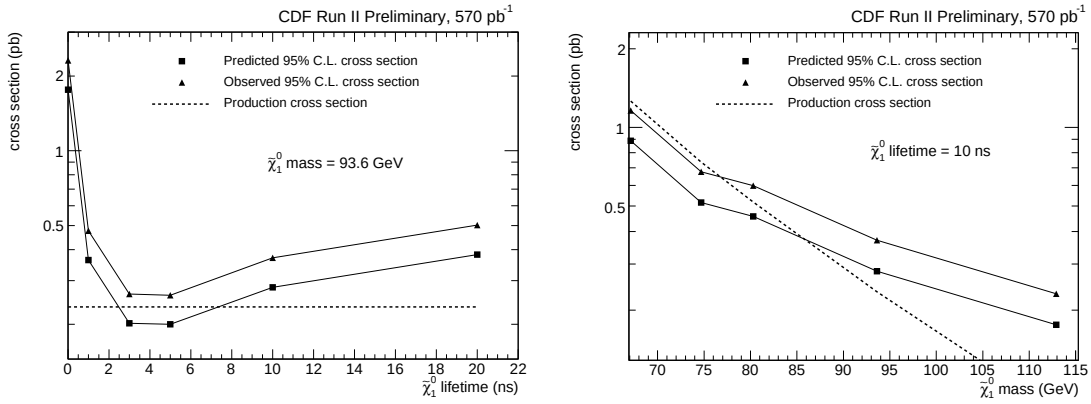

Figure 7: The expected and observed 95% C.L. cross section limit as a function of the $\tilde{\chi}_1^0$ mass (right) and lifetime (left) in our GMSB model.

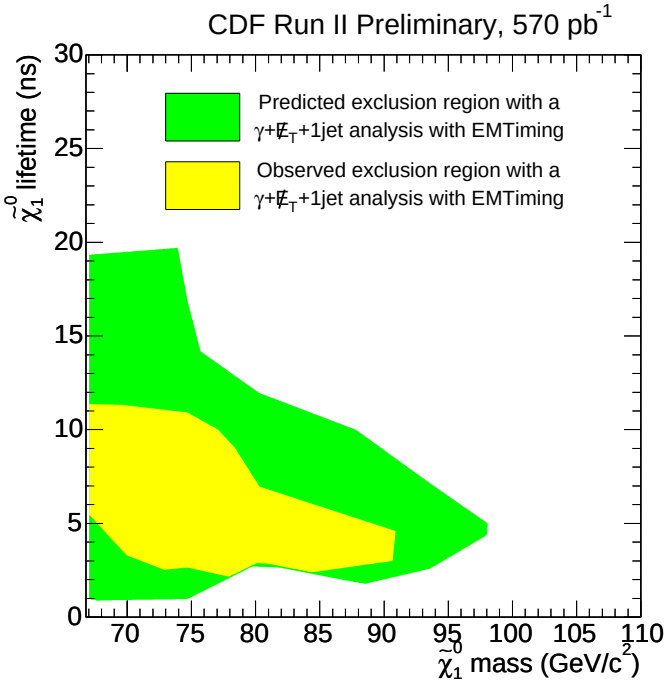

Figure 8: The exclusion region as a function of $\widetilde{\chi}_1^0$ lifetime and mass. We show the exclusion region for the predicted and the observed number of background events.

References

[1] See for example, S. P. Martin, hep-ph/9709356.

[2] M. Goncharov *et. al.*, physics/0512171, accepted for publication in NIM. For more details see http://hepr8.physics.tamu.edu/hep/emtiming/

[3] D. Toback and P. Wagner, Phys. Rev. D **70**, 114032 (2004).

[4] See for example S. Ambrosanio, G. L. Kane, G. D. Kribs, S. P. Martin and S. Mrenna, Phys. Rev. D **54**, 5395 (1996) or C. H. Chen and J. F. Gunion, Phys. Rev. D **58**, 075005 (1998).

[5] F. Abe *et. al.*, (CDF Collaboration), Phys. Rev. Lett. **81** (1998) 1791 and Phys. Rev. D **59** (1999) 092002.

[6] We follow B. C. Allanach *et al.*, Eur. Phys. J. C**25**, 113 (2002), and take the messenger mass scale $M_{\rm M} = 2\Lambda$, $\tan(\beta) = 15$, $\mathrm{sgn}(\mu) = 1$ and the number of messenger fields $N_{\rm M} = 1$. The parameters $c_{\rm Grav}$ (gravitino mass factor) and Λ (supersymmetry breaking scale) are allowed to vary.

[7] ALEPH Collaboration, A. Heister *et. al.*, Eur. Phys. J. C **25**, 339 (2002); A. Garcia-Bellido, Ph.D. thesis, Royal Holloway University of London, 2002 (unpublished), arXiv:hep-ex/0212024.